

LA-UR-02-7695

Approved for public release;
distribution is unlimited.

Title: GEANT simulations for flight path 14

Author(s): R. Reifarth, R.C. Haight, L.F. Hunt, J.L. Ullmann;
LANSCE-3, LANL;
P.E. Koehler Oak Ridge National Laboratory

Submitted to: DANCE project



Los Alamos National Laboratory, an affirmative action/equal opportunity employer, is operated by the University of California for the U.S. Department of Energy under contract W-7405-ENG-36. By acceptance of this article, the publisher recognizes that the U.S. Government retains a nonexclusive, royalty-free license to publish or reproduce the published form of this contribution, or to allow others to do so, for U.S. Government purposes. Los Alamos National Laboratory requests that the publisher identify this article as work performed under the auspices of the U.S. Department of Energy. Los Alamos National Laboratory strongly supports academic freedom and a researcher's right to publish; as an institution, however, the Laboratory does not endorse the viewpoint of a publication or guarantee its technical correctness.

Form 836 (8/00)

GEANT simulations for flight path 14

R. Reifarh^a, R.C. Haight^a, L.F. Hunt^a, P.E. Koehler^b, J.L. Ullmann^a

^a Los Alamos National Laboratory, Los Alamos, New Mexico, 87545, USA

^b Oak Ridge National Laboratory, Oak Ridge, Tennessee, 37831, USA

Abstract

The Detector for Advanced Neutron Capture Experiments (DANCE) is a 159-element 4π barium fluoride array designed to study neutron capture on small quantities. It is being built on flight path (FP) 14, a 20 m neutron flight path, which views the "upper tier" water moderator at the Manuel J. Lujan Jr. Neutron Scattering Center at the Los Alamos Neutron Science Center.

The purpose of the simulations described in this report was twofold. At first the discrepancy between Monte-Carlo simulations carried out with MCNP [1] and neutron flux measurements at FP14 investigated. The next goal was to find possible improvements of the present setup.

The response of the collimation system to neutrons and gamma rays was studied using the Monte Carlo code GEANT 3.21. [2] for different shapes of the last collimator. As a result we suggest to modify the last collimator during the upcoming beam shutdown.

1 Geometry

Between the neutron production target (0 m) and the sample position (20.27 m) a set of four collimators is installed in order to cut down the neutron flux to a radius of about 5 mm. Each of the collimators has a length of about 1 m and consists of a set of 5 % borated polyethylene (B-PE) and copper (Cu) disks. Starting with the most upstream collimator, the inner diameters are decreasing with each step till they reach the smallest values at the final, most downstream collimator.

Figure 1 provides a schematic view of the simulated geometry. In order to check the particle flow during the simulations, five different control layers were defined. The first layer is 3 m downstream of the neutron target, the last one at the sample position and the remaining three between each collimator respectively. These layers were used to check the particle flux as a function of type, energy, time of flight and direction.

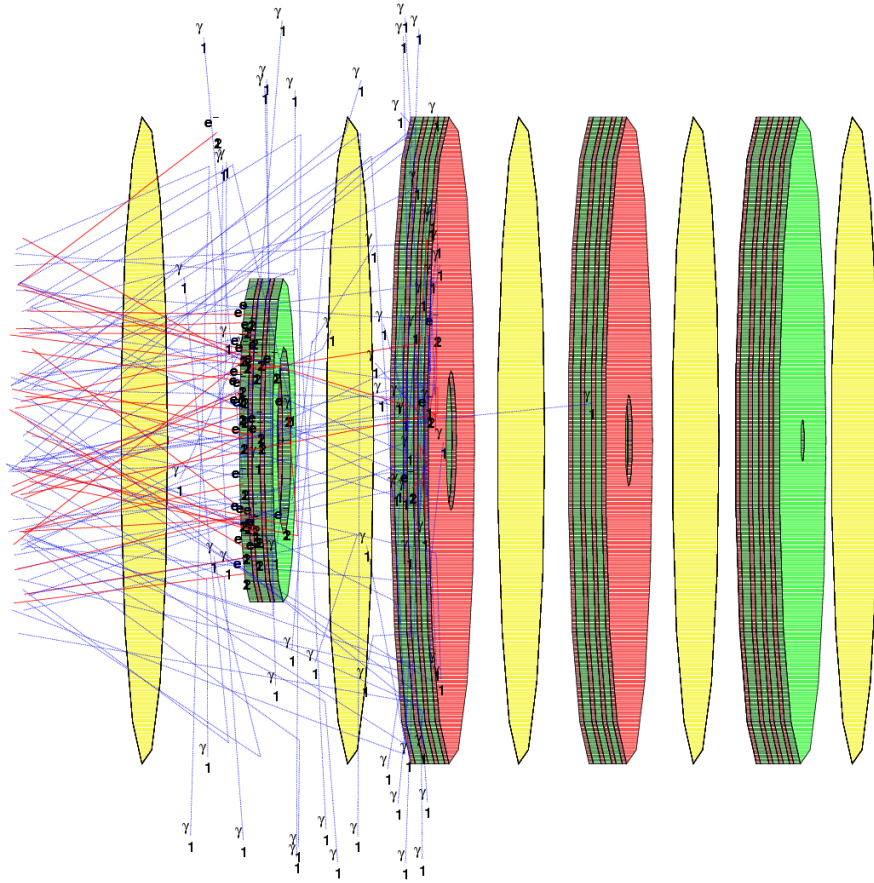


Figure 1: Schematic drawing of the simulated FP14 including the 4 different collimator stages. Each collimator consists of different layers of Cu (green) and borated PE (red). In order to control the different particle fluxes along the beam line, several control layers (yellow) have been included into the simulations. See text for details.

All the important details about the geometry of the first three collimators are listed in Table 1, Table 2, and Table 3.

Table 1: First collimator. The center of the collimator is 600 cm away from the neutron production target. The total length is 80 cm. All position numbers in the table refer to the center of the collimator.

Pos. Upstream (cm)	Pos. Downstream (cm)	Thickness (cm)	Outer radius (cm)	Inner Radius (cm)	Material
-40	-20	20	7.5	4.34	Cu
-20	-10	10	7.5	4.34	B-PE
-10	10	20	7.5	4.34	Cu
10	20	10	7.5	4.34	B-PE
20	40	20	7.5	4.34	Cu

Table 2: Second collimator. The center of the collimator is 1000.5 cm away from the neutron production target. The total length is 91 cm. All position numbers in the table refer to the center of the collimator.

Pos. Upstream (cm)	Pos. Downstream (cm)	Thickness (cm)	Outer radius (cm)	Inner Radius (cm)	Material
-45.5	-35.5	10	15	3.225	B-PE

-35.5	-15.5	20	15	3.225	Cu
-15.5	-4.5	11	15	3.225	B-PE
-4.5	10.5	15	15	3.225	Cu
10.5	20.5	10	15	3.225	B-PE
20.5	35.5	15	15	3.225	Cu
35.5	45.5	10	15	3.225	B-PE

Table 3: Third collimator. The center of the collimator is 1432.5 cm away from the neutron production target. The total length is 91 cm. All position numbers in the table refer to the center of the collimator.

Pos. Upstream (cm)	Pos. Downstream (cm)	Thickness (cm)	Outer radius (cm)	Inner Radius (cm)	Material
-45.5	-35.5	10	15	2.1	B-PE
-35.5	-15.5	20	15	2.1	Cu
-15.5	-5.5	10	15	2.1	B-PE
-5.5	10.5	16	15	2.1	Cu
10.5	20.5	10	15	2.1	B-PE
20.5	35.5	15	15	2.1	Cu
35.5	45.5	10	15	2.1	B-PE

The last collimator is about 100 times longer than wide. This implies a crucial influence of the shape of the inner diameter to the collimation. Additionally, the inner set of this collimator can be changed without major constructions at the flight path, since it is accessible from the experimental room after removing the vacuum system. Therefore three different solutions for the last collimator have been investigated. The changes investigated within this report affect only the inner diameters of the different layers of the last collimator. The thicknesses as well as the materials were left unchanged. Figure 2 provides a schematic view of the different simulated shapes. The straight version is presently (October 2002) realized. The two different conical shaped solutions are optimized in terms of neutrons per unit area at the sample position. As it turned out, the present solution reduces not only the neutron flux outside the nominal sample radius, but also the neutron flux at very small sample radii. The reason for this reduction is that the collimator is so small, that no point at the sample position is irradiated by the whole neutron target.

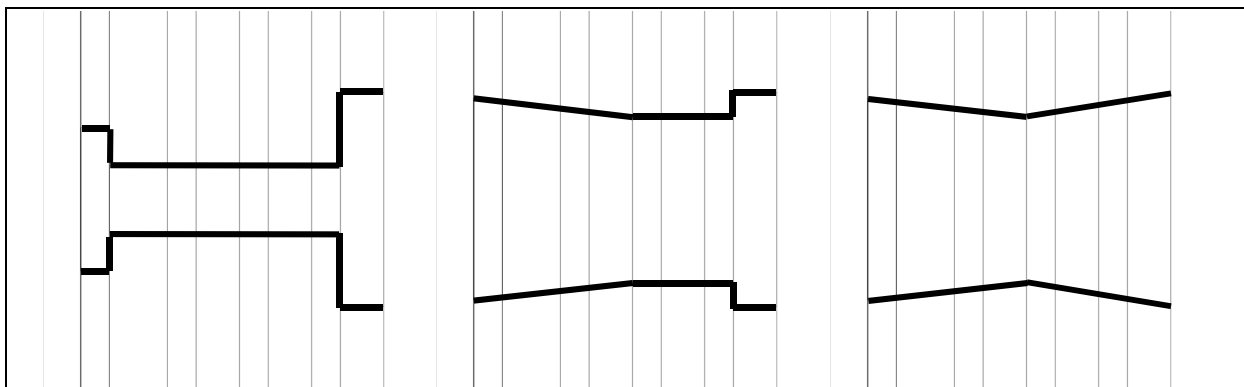


Figure 2: Schematic view of the three different configurations of the last collimator. The neutrons are traveling from left to right. The thick lines correspond to the shape of the hole inside the collimator. The details of the straight (left), conical (middle), and biconical (right) shape are described in the text. The straight as well as the conical version contain so-called “clean up” collimators. Such collimators are frequently used and have a greater radius than the nominal beam radius at the actual position.

The conical as well as the biconical shape correspond to the idea, that the whole sample of radius $r_{\text{sample}} = 0.25$ cm at a distance $d_{\text{sample}} = 20.2$ m is irradiated by the whole moderator with radius $r_{\text{moderator}} = 6$ cm. The inner radius as a function of the distance (d) from the moderator of upstream half of both versions follows therefore:

$$f_{\text{core}} = \frac{r_{\text{moderator}} - r_{\text{sample}}}{d_{\text{sample}}},$$

$$r_{\text{collimator}} = (d_{\text{sample}} - d_{\text{collimator}}) \cdot f_{\text{core}} + r_{\text{sample}}.$$

While the downstream half of the conical solution stays straight, the biconical is designed to follow the lines of the penumbra:

$$f_{\text{penumbra}} = \frac{r_{\text{moderator}} + r_{\text{change}}}{d_{\text{change}}}, \quad r_{\text{collimator}} = (d_{\text{collimator}} - d_{\text{change}}) \cdot f_{\text{penumbra}} + r_{\text{change}},$$

where r_{change} and d_{change} refer to the radius and the distance from the sample, where the slope changes, respectively.

The details about the three different shapes of the last collimator are listed in Table 4, Table 5, and Table 6 and shown in Figure 3, Figure 4, and Figure 5.

Table 4: Fourth collimator, straight realization. The center of the collimator is 1849.85 cm away from the neutron production target. The total length is 106.7 cm. All position numbers in the table are relative to the center of the collimator.

Pos. Upstream (cm)	Pos. Downstream (cm)	Thickness (cm)	Outer radius (cm)	Inner Radius upstream (cm)	Inner Radius downstream (cm)	Material
-53.35	-43.15	10.2	15	0.635	0.635	B-PE
-43.15	-22.85	20.3	15	0.300	0.300	Cu
-22.85	-12.75	10.1	15	0.300	0.300	B-PE
-12.75	2.55	15.3	15	0.300	0.300	Cu
2.55	12.65	10.1	15	0.300	0.300	B-PE
12.65	27.95	15.3	15	0.300	0.300	Cu
27.95	38.05	10.1	15	0.300	0.300	B-PE
38.05	53.35	15.3	15	0.950	0.950	Cu

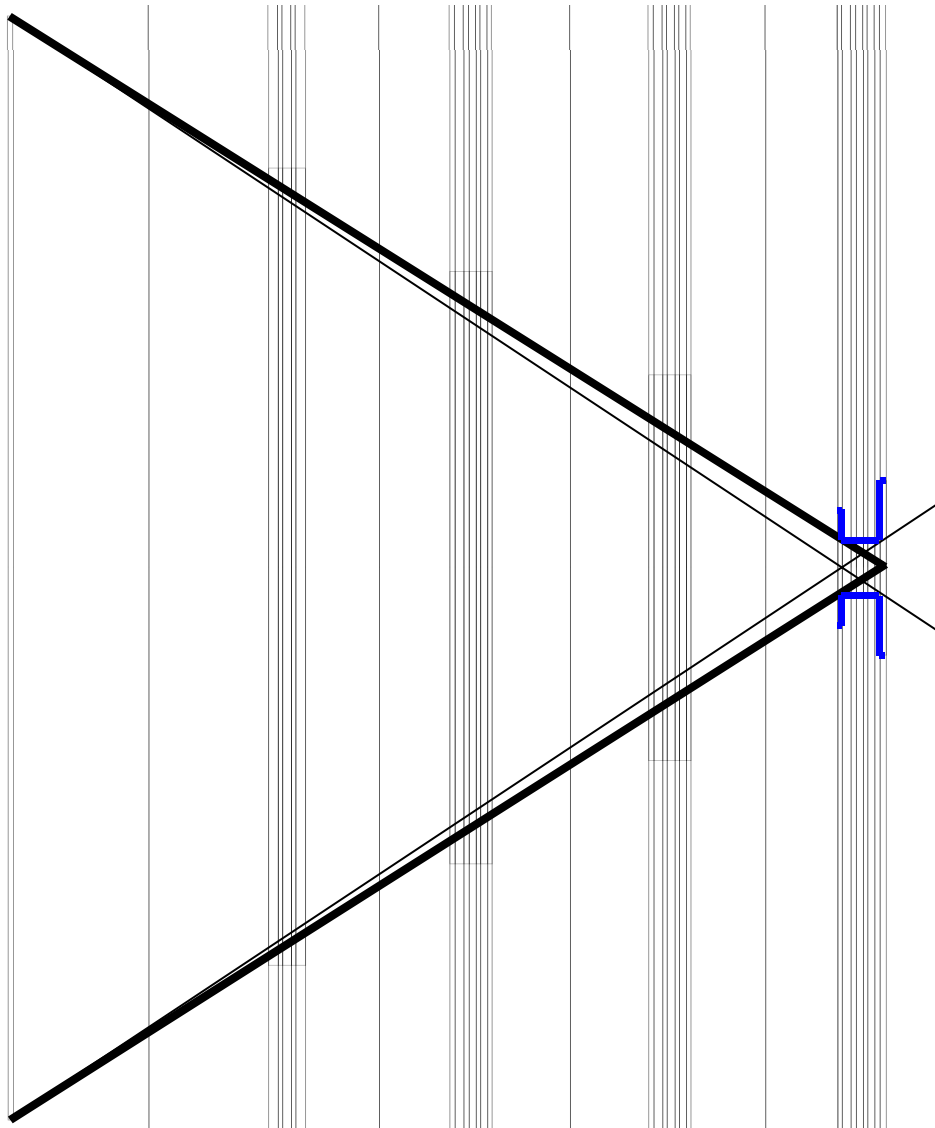


Figure 3: Sketch of the whole beam line with the straight collimator. The vertical axis is magnified by a factor of 20, otherwise the drawing is on scale. The inner shape of the last collimator is shown in blue. The thick black line corresponds to the umbra, while the slightly thinner black line shows the penumbra. Obviously the whole sample position (last single line to the right) is in the penumbra region.

Table 5: Fourth collimator, conical realization. The center of the collimator is 1849.85 cm away from the neutron production target. The total length is 106.7 cm. All position numbers in the table refer to the center of the collimator.

Pos. Upstream (cm)	Pos. Downstream (cm)	Thickness (cm)	Outer radius (cm)	Inner Radius upstream (cm)	Inner Radius downstream (cm)	Material
-53.35	-43.15	10.2	15	0.894	0.864	B-PE
-43.15	-22.85	20.3	15	0.864	0.806	Cu
-22.85	-12.75	10.1	15	0.806	0.777	B-PE
-12.75	2.55	15.3	15	0.777	0.733	Cu
2.55	12.65	10.1	15	0.733	0.733	B-PE
12.65	27.95	15.3	15	0.733	0.733	Cu
27.95	38.05	10.1	15	0.733	0.733	B-PE
38.05	53.35	15.3	15	0.950	0.950	Cu

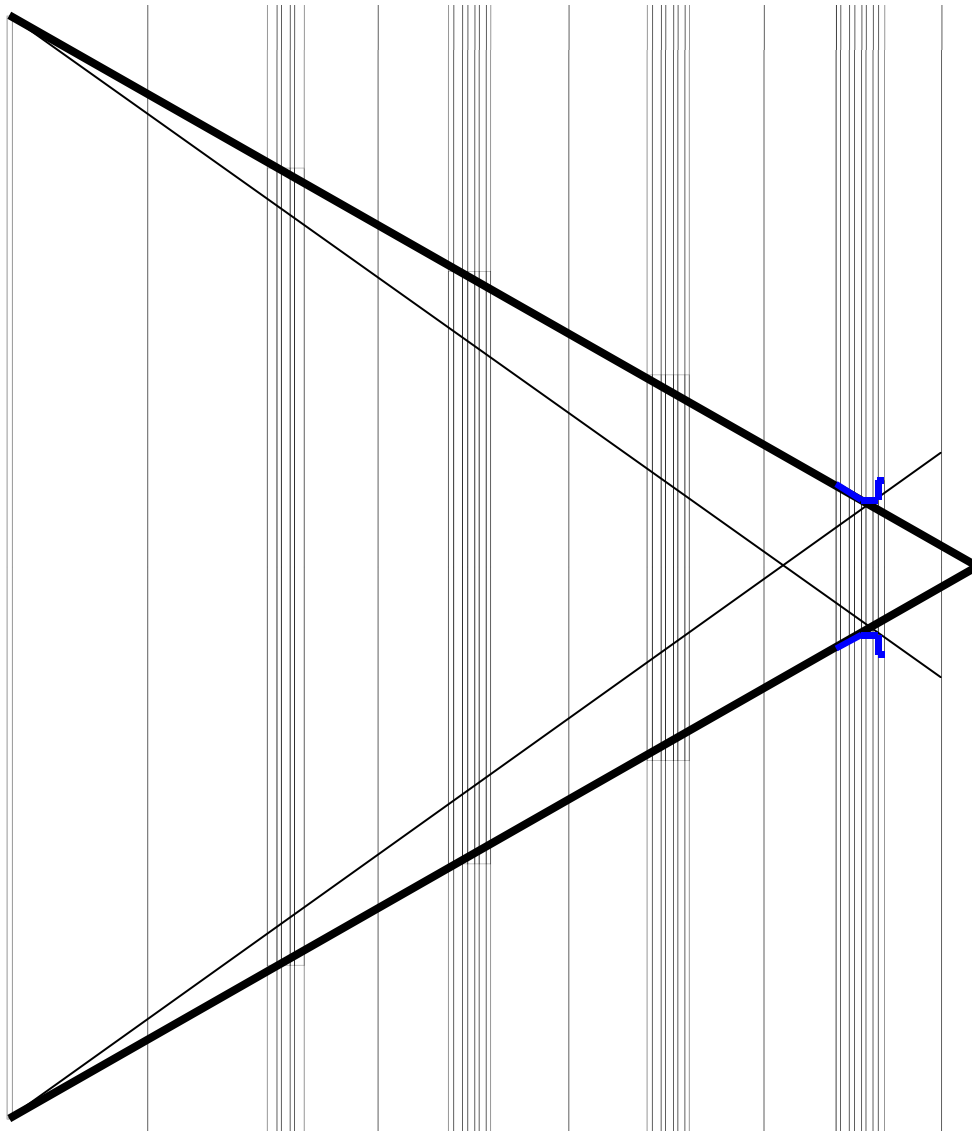


Figure 4: Sketch of the whole beam line with the conical collimator. The vertical axis is magnified by a factor of 20, otherwise the drawing is on scale. The inner shape of the last collimator is shown in blue. The thick black line corresponds to the umbra, while the slightly thinner black line shows the penumbra. The inner part of the sample position (last single line to the right) is in the umbra region and has therefore a constant neutron flux.

Table 6: Fourth collimator, biconical realization. The center of the collimator is 1849.85 cm away from the neutron production target. The total length is 106.7 cm. All position numbers in the table refer to the center of the collimator.

Pos. Upstream (cm)	Pos. Downstream (cm)	Thickness (cm)	Outer radius (cm)	Inner Radius upstream (cm)	Inner Radius downstream (cm)	Material
-53.35	-43.15	10.2	15	0.894	0.864	B-PE
-43.15	-22.85	20.3	15	0.864	0.806	Cu
-22.85	-12.75	10.1	15	0.806	0.777	B-PE
-12.75	2.55	15.3	15	0.777	0.733	Cu
2.55	12.65	10.1	15	0.733	0.733	B-PE
12.65	27.95	15.3	15	0.733	0.774	Cu
27.95	38.05	10.1	15	0.774	0.836	B-PE
38.05	53.35	15.3	15	0.836	0.877	Cu

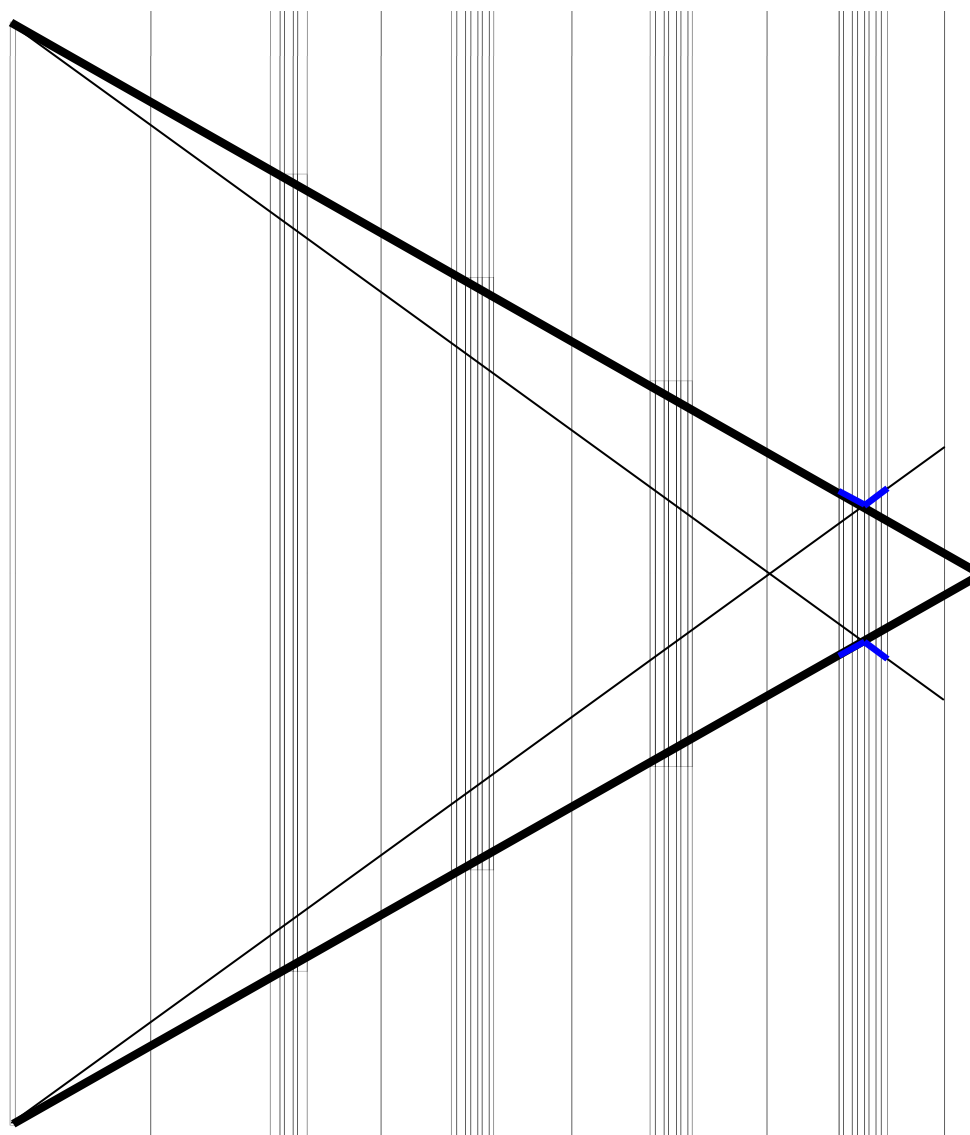


Figure 5: Sketch of the whole beam line with the conical collimator. The vertical axis is magnified by a factor of 20, otherwise the drawing is on scale. The inner shape of the last collimator is shown in blue. The thick black line corresponds to the umbra, while the slightly thinner black line shows the penumbra. The inner part of the sample position (last single line to the right) is in the umbra region and has therefore a constant neutron flux.

2 Simulations with γ -rays

Low energetic γ -rays of 55 keV have been traced starting at the position of the neutron moderator. Whenever these photons interact with the beam pipe or with the collimators their energy falls below the GEANT-internal cut-off energy of 50 keV and they are not traced anymore. The results of these simulations can therefore be interpreted as images of the neutron target seen at different positions along the flight path.

2.1 Discrepancy between MCNP and experiment

Within this report only the neutron transport along FP14 was simulated. The neutron flux emitted by the neutron production target was taken from MCNP calculations. Former estimations of the neutron transport along the flight path could be confirmed. Assuming a $1/E$ spectrum, the integrated number of neutrons per energy decade is constant and therefore a reasonable unit.

$$\int_{E_0}^{10 \cdot E_0} \Phi_n(E) dE = \int_{E_0}^{10 \cdot E_0} \text{const} \cdot \frac{1}{E} dE = \text{const} \cdot \ln(10)$$

The expected flux at the target position with the straight collimator should be:

$$\mathbf{3.58 \cdot 10^3 \text{ neutrons / s / neutron energy decade / } \mu\text{A}}$$

Actual measurements of the neutron flux at FP14 brought up a reduced flux by a factor of 5 compared to the simulations carried out so far. A possible explanation could be a slight displacement of the last collimator within the uncertainties of the alignment procedure. In order to check this possible explanation in detail, two simulations have been carried out.

At first the whole collimator was moved perpendicular to the beam axis by 3 mm. This displacement resulted in a shift of the beam spot at the sample position, but no reduction of the neutron flux could be seen. An misalignment of 3 mm is well within the uncertainties.

In the second simulation the collimator was tilted by 0.2 degrees, while the center of the collimator was kept in place, which corresponds to a misalignment of 3.5 mm of one collimator end with respect to the other end. This resulted also in a flux reduction of about a factor two (61 %). This implies a strong dependence of the neutron flux on the position of one end of the 4th collimator, while the respective other end stays in place. First experimental results confirm this trend (Figure 6). The final alignment will be prepared during the upcoming shutdown and will be carried out at the beginning of the beam period 2003.

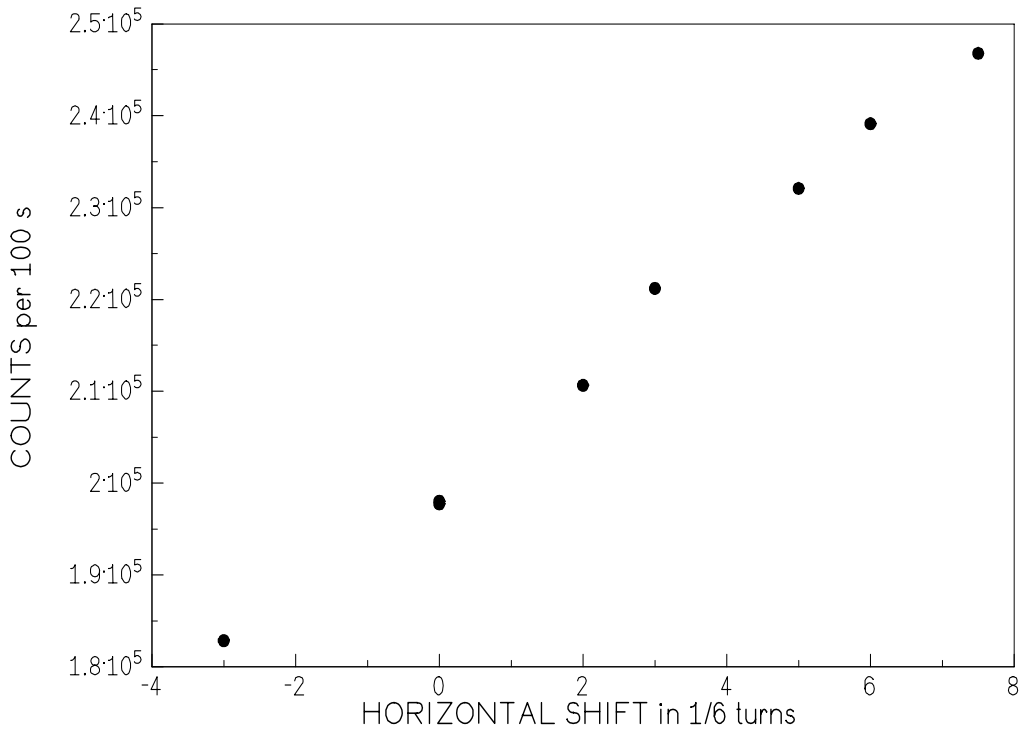


Figure 6: Experimental results of the horizontal displacement of the downstream end of the last collimator. One turn corresponds to a shift of about 2 mm. Measured is the count rate of a BaF₂ crystal perpendicular to the beam with a polyethylene piece in the neutron beam.

2.2 Different geometries for collimator 4

Figure 7 shows the results of the three different versions of the last collimator. 10^8 γ -rays have been started at the position of the neutron target. The gammas were emitted uniformly from a disk with a radius of 6 cm, which corresponds approximately to the size of the water moderator, which acts as the neutron emission area for FP14. In order to save CPU-time, the emission angle relative to the direction of the beam line was restricted to 0.5 degrees, which means, that the maximum travel of the gammas perpendicular to the beam line is a 17 cm for 20 m flight path. With a nominal sample radius of 0.25 cm, all versions show a plateau of constant number of gammas per area up to 0.4 cm, which is preferable, since the mass distribution of the sample might not be uniform. The gamma flux of the conical realizations is increased by a factor of 4.5 compared to the straight version. The trade off is an increased halo-region: 1.3 cm compared to 0.8 cm. The beam profiles of the two different conical solutions are the same up to 1 cm radius, while the outer halo region of the biconical version is somewhat bigger than the one of the conical version. This implies, that at this point the conical configuration is to prefer over the biconical one.

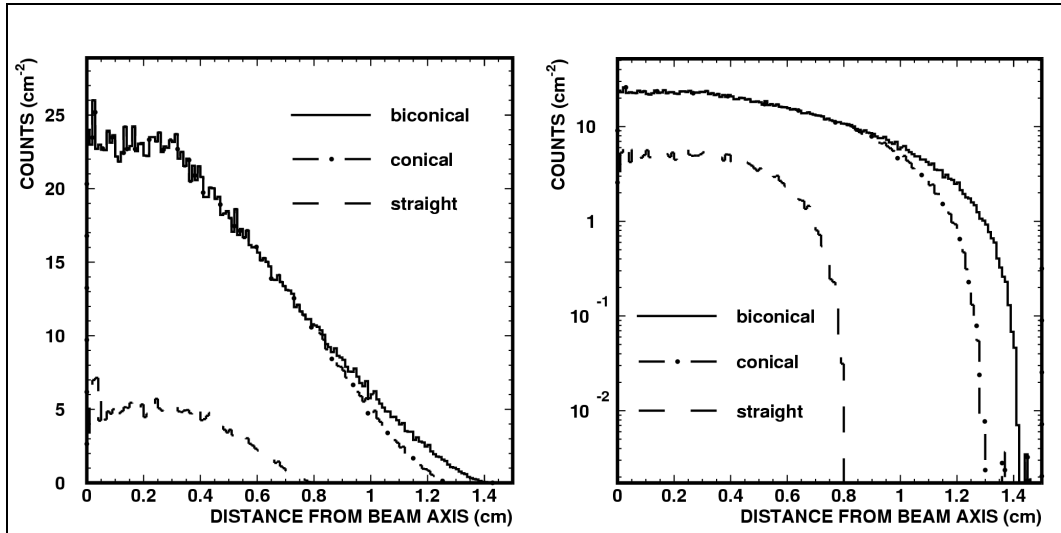


Figure 7: Results of simulations of γ -ray with energies of 55 keV. Both pictures contain the same data. The y-axis of the left one is linear, while the right one is in logarithmic scale.

3 Simulations with neutrons

Neutrons don't behave like low energetic photons in a sense that they usually do not disappear after an interaction. The most likely interaction of a neutron with energies above 1 keV, and especially above 1 MeV, is elastic or inelastic scattering. Therefore additional simulations are needed in order to investigate these extra effects (please see also Sect. 3.2).

In a first attempt neutrons with an $1/E$ energy dependence were simulated. Starting at the neutron moderator 10^7 neutrons per decade between 1 eV and 100 MeV were emitted. The beam started with 6 cm radius and an opening angle of 0.5 degrees. High-energy neutrons showed a significant extra background component at the sample position. Therefore the results of low-energy neutrons will be discussed in the next section (3.1), while the high energetic neutrons will be discussed in section 3.2.

3.1 Low-energy neutrons

Neutrons below 100 keV will usually be stopped shortly after the first interaction. Since scattering cross sections as well as (n,x) cross sections increase very quickly with decreasing neutron energy, these neutrons will be stopped by producing γ -rays or charged particles very close to the first interaction point. Therefore the expected beam profile at the sample position is similar to the profile derived by simulating low energetic γ -rays. Figure 8 shows a representative result for neutrons with energies between 1 and 10 keV. A comparison with Figure 7 confirms the discussion above.

Since the situation will be different for high-energy neutrons, it is important to point out, that the neutron flux for distances greater than 1.5 cm from the center of the beam axis is reduced by more than 5 orders of magnitude.

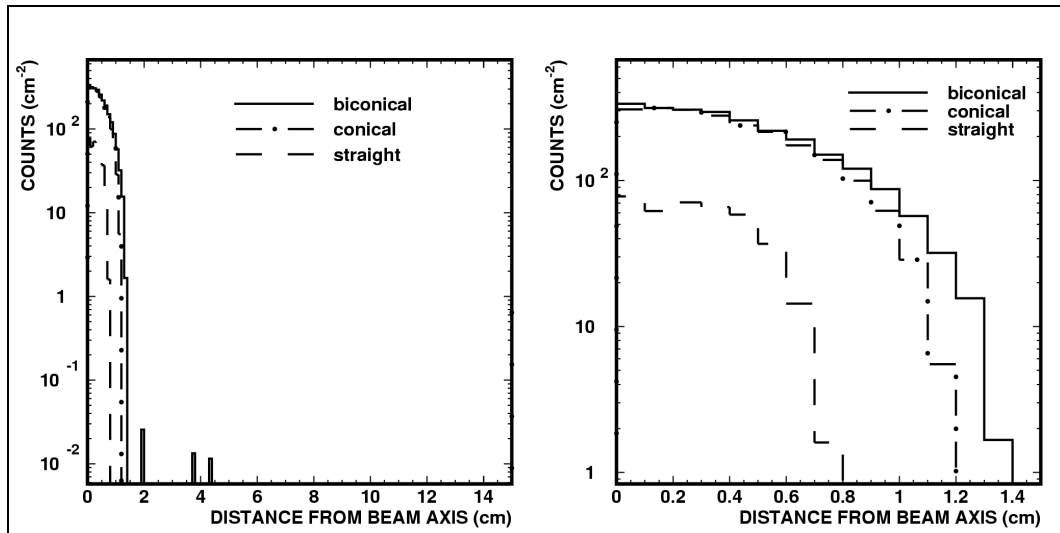


Figure 8: Results of simulations of neutrons with energies between 1 and 10 keV. Both pictures contain the same data. The x-axis of the left one shows the whole region of interest up to 15 cm radius, while the right one shows only the region very close to the neutron beam allowing to compare the neutron profiles at the sample position. 10^7 neutrons were started at the neutron moderator.

3.2 High-energy neutrons

Neutrons above 1 MeV are very difficult to shield. Depending on the material, the main interaction mechanism is elastic or inelastic scattering on nuclei. While the energy loss during inelastic neutron scattering can be significant, the cross sections are usually very small except for a small energy region just above the excitation energy of the respective nucleus. In contrary, elastic scattering cross sections are usually fairly big over a broad energy range, while the energy loss is very small. This implies, that a high energy neutron will interact many times before it will be captured eventually. Figure 9 shows the result of a simulation with neutrons between 10 and 100 MeV energy. In order to improve the statistics 10^8 neutrons were simulated. Obviously the beam profile close to the center of the beam is the same as for low energetic neutrons. However, with increasing distance to the beam center, the beam profile shows significant differences.

In the region between 1.5 and 5 cm a beam halo, with a neutron flux 3 to 4 orders of magnitude smaller than the flux in the center of the beam, appears. This beam halo originates from neutrons coming directly from the moderator and being scattered once inside the last collimator.

Another remarkable component appears at even higher radii. A flat plateau, with a neutron flux 5 orders of magnitude below the center flux, extends up to the highest simulated radius of 15 cm.

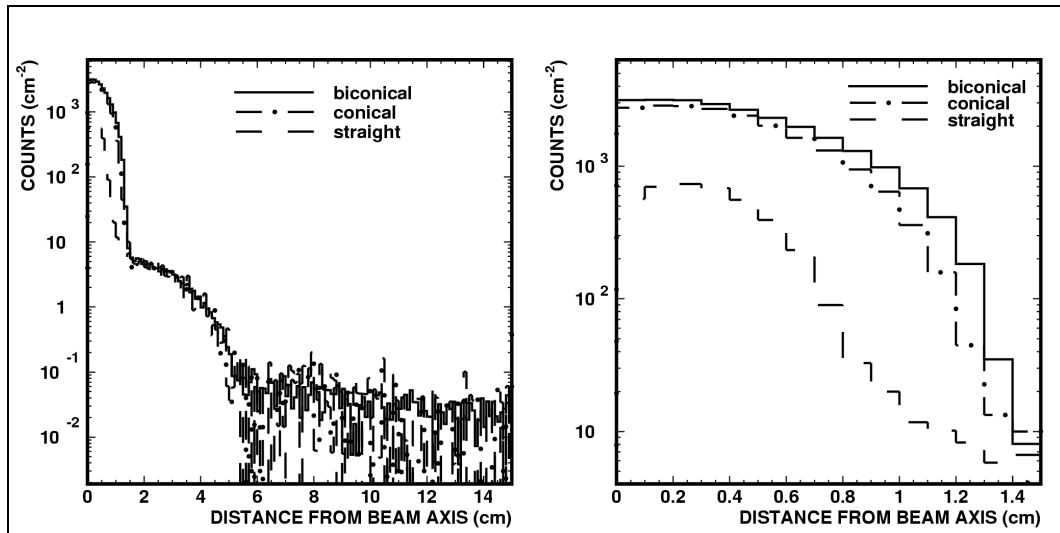


Figure 9: Results of simulations of neutrons with energies between 10 and 100 MeV. Both pictures contain the same data. The x-axis of the left one shows the whole region of interest up to 15 cm radius, while the right shows only the region very close to the neutron beam allowing to compare the neutron profiles at the sample position. 10^8 neutrons were started at the neutron moderator.

4 Conclusions

Close to the target the conical geometries provide a neutron flux which is almost a factor of 5 higher than for the straight geometry. This would imply a significantly improved signal to not beam related background ratio as well as much improved statistics for the same run time. Both conical solutions show a broader beam profile than the straight one, the profile of the single conical solution being slightly narrower. If the geometrical size of the sample is limited to a few millimeter, while the backing can not be made of the same size, a narrow beam halo might be more important than a higher neutron flux.

At a distance of more than 1.5 cm from the beam axis there is no difference between the 3 solutions anymore. Especially for high energetic neutrons the collimation of the last collimator has no influence.

Therefore, we suggest to prepare conical insets for the last collimator in order to install and test them during the next shutdown period. Which set of collimators is actually used might depend on the geometry of the actual sample.

5 References

- [1] G.J. Russell, *private communication*.
- [2] Apostolakis, J., (1993), *Tech. Rep. CERN*, GEANT library (1993), www.cern.ch.